IEEE Access
Multidisciplinary | Rapid Review | Open Access Journal

Received January 24, 2019, accepted February 14, 2019, date of publication February 25, 2019, date of current version March 12, 2019.

Digital Object Identifier 10.1109/ACCESS.2019.2901377

Modeling of Supercapacitor Behavior With an Improved Two-Branch Equivalent Circuit

DAN XU, LE ZHANG, BIN WANG, AND GUANGLIANG MA
State Key Laboratory for Manufacturing Systems Engineering, Xi'an Jiaotong University, Xi'an 710049, China

Corresponding author: Bin Wang (wangbin8751@xjtu.edu.cn)

This work was supported in part by the Postdoctoral Science Foundation of China under Grant 2018M631143, in part by the National Natural Science Foundation of China under Grant 21808179, and in part by the Nature Science Basic Research Plan in Shaanxi Province of China under Grant 2018JQ5126.

ABSTRACT In this paper, an improved two-branch equivalent circuit model with a controlled current source is proposed to describe the real-time charge/discharge and self-discharge operating characteristics of a supercapacitor (SC). First, the self-discharge mechanism of the SC is investigated based on the two-branch model and experimental analyses at the different charge and discharge stages. Furthermore, the controlled current source is introduced into the two-branch model to reflect the self-discharge effect of the SC. On this basis, the recursive least square method is adapted to identify the model parameters. To improve the accuracy of the proposed model, the iterative optimization algorithm is also adapted to optimize the dynamic parameters of the controlled current source. Finally, the improved two-branch equivalent circuit model with the controlled current source is simulated. The simulation results are basically in accordance with the experimental results. The relative error of the proposed model is less than 0.7%. Compared with the conventional two-branch model, the proposed model can not only reflect the SC dynamic behavior during the charge/discharge phase but also better reflect the self-discharge effect of the SC.

INDEX TERMS Supercapacitor, equivalent circuit model, self-discharge effect, controlled current source, parameters identification.

I. INTRODUCTION

Supercapacitors (SCs) are being actively and widely studied in recent years since they represent a promising new energy storage technology [1], [2]. Compared with conventional batteries and capacitors, SCs have comprehensive advantages of high power density and high expected reliability. In addition, SCs can be discharged and charged more efficiently and quickly, and have longer cycle life than that of conventional batteries. Therefore, SCs have been widely employed in energy storage systems (ESSs) of electric vehicles (EVs) [3], [4], solar/wind generation power systems [5], [6], wireless sensor nodes [7], [8], etc. In ESSs applications, they usually use SC terminal voltage as the feedback of controller to achieve real-time control for the SC. However, the SC terminal voltage would be affected by many factors [9]–[11]. To effectively evaluate the SCs terminal voltage and achieve the precise control for the SCs in the ESSs, it is crucial to establish an accurate model for the SC [11], [12].

The associate editor coordinating the review of this manuscript and approving it for publication was Norbert Herencsar.

The SC has a special structure with double-layer capacitance such that it has an excellent fast charge and discharge performance [13]. However, a complex self-discharge or potential voltage recovery phenomenon cannot be avoided with this special structure [14]. The self-discharge effect is characteristic of nonlinearity. So it is difficult to use a simple model to describe the self-discharge effect of the SC. In previous studies, it has been widely accepted that the self-discharge process is presented with three mechanisms: the faradaic charge-transfer reaction, the diffusion-controlled faradaic redox reaction and the leakage current [15]–[17]. Generally, the faradaic charge-transfer reaction occurs when the SC is overcharged. With the diffusion-controlled faradaic process, instability of faradaic response caused by the redox reaction cannot be avoided. In addition, the leakage current always occurs since the SC has an internal ohmic leakage pathway. In practical applications, the self-discharge of the SC could not be ignored since it might affect the real-time charge and discharge behaviors (it is related to the SOC). And not only that, the self-discharge characteristics of the SC are also related to external factors such as initial voltage

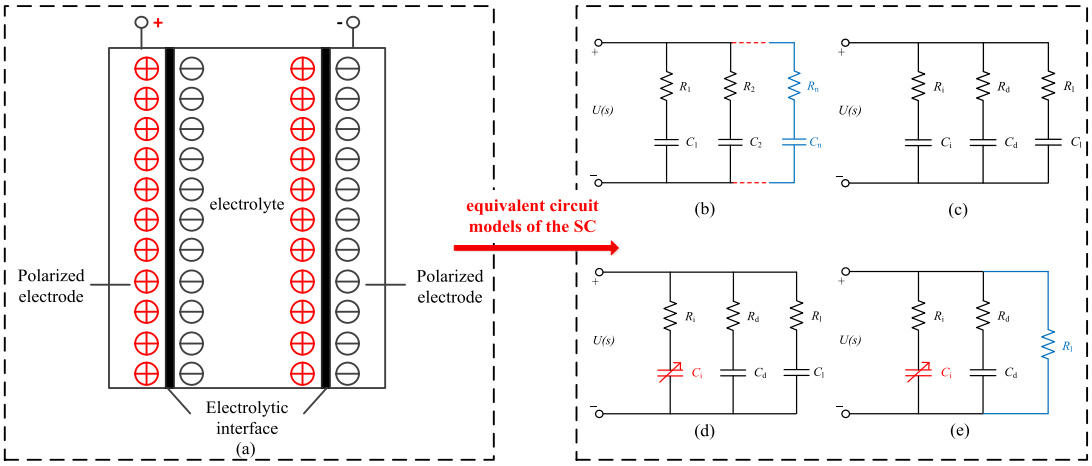

FIGURE 1. Structure and equivalent circuit models of the SC. (a) Schematic diagram of the SC. (b) Multi-branch equivalent circuit model. (c) Three-branch equivalent circuit model. (d) Equivalent circuit model with a variable capacitance. (e) Equivalent circuit model with a parallel leakage resistance.

and charging period [18], [19], etc. For these reasons, the precise self-discharge description is of critical importance for establishing the accurate model of the SC.

To describe the self-discharge performance of the SC, the equivalent circuit model with a controlled voltage source or a variable leakage resistance has been studied, respectively [16], [17]. The SC model with the controlled voltage source can effectively reflect the nonlinear characteristics of the SC. Besides, it can also reflect the self-recovery performance of the SC terminal voltage at the end of charge and discharge stages. However, it cannot simulate the superposition current effect caused by the internal charge diffusion reaction of the SC during the static stages. What's worse, the controlled voltage source would be coupled with the SC terminal voltage, which would increase the computational complexity of the model in practical applications. The SC model with the variable leakage resistance can reflect the dynamic self-discharge characteristics of the SC [16]. However, the estimation of the variable leakage resistance involves a complex exponential operation. Moreover, if the parameters of the dynamic variable leakage resistance in the self-discharge branch could not be updated in time, an unexpected calculation error could not be avoided [20], [21]. Although the models with comprehensive CPE or Warburg can effectively mimic the self-discharge behavior of the SC, they cannot reflect the elementary phenomena of the residual charge redistribution [12], [22], [23].

In [24], an equivalent circuit model with a controlled current source was established to reflect the real-time operating performance of the SC during the charge/discharge and rest stages. The controlled current source can reflect the superimposed current effect of the SC residual charge and compensate the SC terminal voltage at self-discharge stages. However, the complex self-discharge effect in accordance with the SC terminal voltage dynamic (i.e., the change rate of the SC terminal voltage) was not fully considered. In addition, the model accuracy is still not perfect in practical applications. In this paper, the two-branch equivalent circuit model is improved based on a controlled current source with two dynamic parameters. The design of the controlled current source takes into account the SC terminal voltage and terminal voltage dynamic, which can effectively describe the real-time self-discharge performance of the SC. Then, the recursive least square algorithm is adopted to identify parameters of the proposed model. To improve the model precision, the iterative optimization algorithm is adopted to modify the parameters of the controlled current source. Based on the improved two-branch model with the controlled current source and the parameters identification method, the SC self-discharge performance can be effectively described, and the model accuracy can be improved.

This paper is organized as follows. Section II presents the multi-branch equivalent circuit model and studies the conventional two-branch model of the SC in detail. In Section III, the improved two-branch equivalent circuit model with the controlled current source is designed. In Section IV, the recursive least square algorithm and the iterative optimization algorithm are employed to achieve the model parameters identification and the optimization of the controlled current source, respectively. Section V discusses the simulation and experimental results. Conclusions are given in Section VI.

II. EQUIVALENT CIRCUIT MODEL OF THE SC

The schematic diagram of the SC and its equivalent circuit models are shown in Fig. 1. In Fig. 1(b), the multi-branch equivalent circuit model of the SC is presented. It can be seen that every branch includes the equivalent series capacitance and resistance. For the multi-branch circuit model of the SC, each of the branches can represent different behaviors of the SC at different times. For example, the branches of a three-branch model can represent the immediate, short-time and long-time behaviors of the SC. The more branches are employed, the higher precision can be achieved with the multi-branch equivalent circuit model. However, the

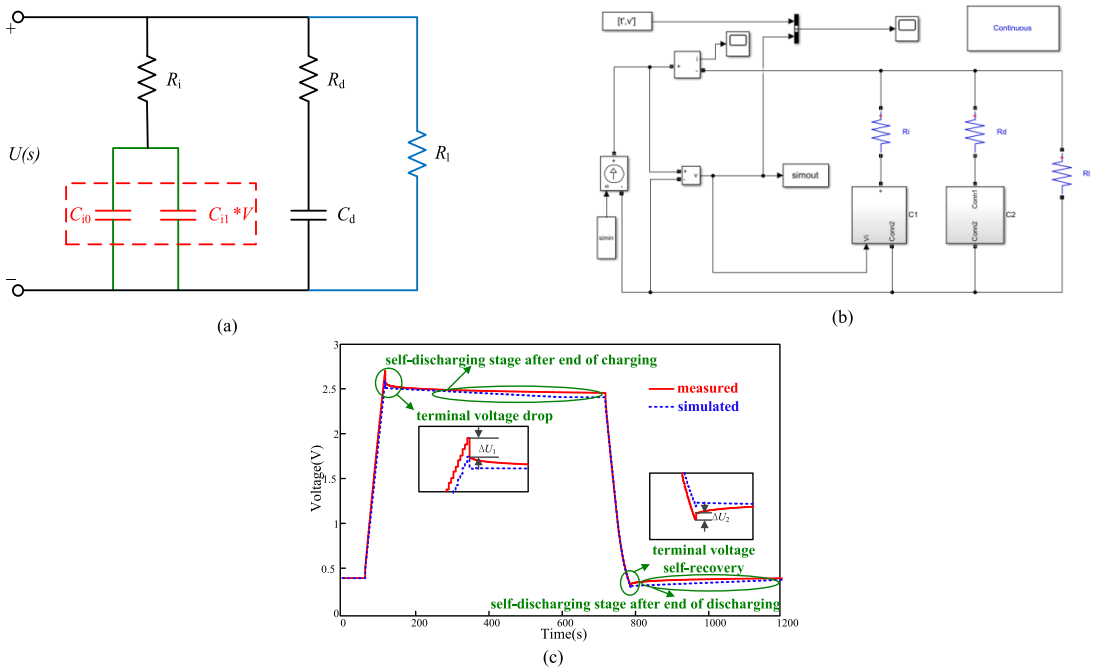

FIGURE 2. Two-branch model with the parallel leakage resistance and simulation results. (a) Two-branch model. (b) Simulation model. (c) Comparative results of the simulation and experiment.

multi-branch equivalent circuit model would not be so easy to implement with lots of branches [25]–[27]. Therefore, the two-branch and three-branch equivalent circuit models have been widely used in practical applications since they can be easily implemented.

The classical three-branch equivalent circuit model is shown in Fig. 1(c). To better reflect the variable capacitance in accordance with the load voltage variation of the SC, Faranda [25] adopted a variable capacitance C_i and an equivalent series resistance R_i in the first branch of the three-branch model, as shown in Fig. 1(d). With this model, the dynamic relationship between the terminal voltage and the variable capacitance of the SC could be reflected in real time. However, compared with the classical three-branch equivalent circuit model, the parameters identification would become more complex since C_i changes in real time during the charge and discharge processes [29].

Based on the three-branch structure, many improved SC equivalent circuit models were proposed [25], [30], [31]. In order to reflect the self-discharge performance of the SC, some researchers proposed the two-branch model with a parallel leakage resistance [25], [30], as shown in Fig. 1(e). In this model, the parallel leakage resistance R_l can effectively reflect the self-discharge process of the SC. But it is challenging for the design of the R_l. If the parameter R_l is designed with a constant value, the variable self-discharge effect of the SC cannot be accurately expressed [32]. On the contrary, if the parameter R_l is designed as a variable value, the variable parameter R_l should be designed as a function of the SC terminal voltage and current [16], [31]. What's more, the parallel leakage resistance would interact with the equivalent series resistances and capacitances of other branches in the model. In summary, the two-branch model with the variable leakage resistance would also increase the complexity of the parameters identification.

To study the two-branch model with the parallel leakage resistance, a specific simulation model is established in Matlab/Simulink, as shown in Fig. 2. Notice that the variable capacitance C_i in the first branch is replaced by a constant capacitance C_{i0} and a voltage-based capacitance $C_{i1} * V$, in which V is in accordance with the SC terminal voltage. By using this model, the time-varying charge and discharge processes could be effectively described with the first branch, especially for the fast charge and discharge characteristics of the SC. Moreover, R_i, C_{i0}, C_{i1} and R_l in the two-branch model can be easily identified since they could be designed with constant values.

To identify the parameters of the two-branch model with the parallel leakage resistance, an experiment is also implemented. In the experiment, the SC initial voltage is designed as 0.4 V, the constant charge/discharge current is set as 15 A. The SC is kept in a static state for 10 minutes after the end of charging and discharging, respectively. The purpose is to reflect the middle-term self-discharge behavior of the SC in practical applications. The parameters of the two-branch model are identified by the recursive least square method. The results are presented in Table 1. The comparative results of the simulation and experiment are shown in Fig. 2(c).

It can be seen from Fig. 2(c) that the two-branch model can effectively reflect the charge and discharge characteristics

TABLE 1. Parameters identification results of the two-branch model.

Parameters	Unit	Identification results
R_i	Ω	0.0081
R_d	Ω	0.0643
R_l	Ω	30.1273
C_{i0}	F	378.0197
C_{i1}	F/V	0.1248
C_d	F	9.4129

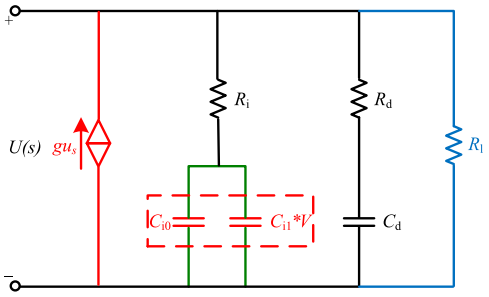

FIGURE 3. The improved two-branch equivalent circuit model with a controlled current source.

of the SC. It also means that the parameters R_i, C_{i0}, C_{i1}, R_d and C_d can describe the SC characteristics. However, the middle-term self-discharge effect of the SC cannot be reflected completely. Furthermore, the relative error of the two-branch model is up to 1.78%. Therefore, the two-branch model is insufficient to describe the self-discharge behavior of the SC. To address the above issues, an improved two-branch equivalent circuit model with a controlled current source is proposed for the SC based on the two-branch model with the parallel leakage resistance.

III. IMPROVED TWO-BRANCH EQUIVALENT CIRCUIT MODEL WITH A CONTROLLED CURRENT SOURCE

A. DESIGN OF THE CONTROLLED CURRENT SOURCE

Based on the above section, it can be known that the SC terminal voltage would drop obviously after the end of charging [17], [33]. On the contrary, the self-recovery phenomenon of the SC terminal voltage would occur after the end of discharging. Therefore, the self-discharge effect of the SC would affect its terminal voltage at different operating stages. Moreover, it can be seen from Fig. 2(c) that the self-discharge effect also has an effect on the change rate of the SC terminal voltage.

In [24], an equivalent circuit model with the controlled current source is proposed for modeling the SC dynamic. But the dynamic relationship among the SC self-discharge and the change rate of the SC terminal voltage cannot be effectively reflected. So the equivalent circuit model with the controlled current source is improved by considering the change rate of the SC terminal voltage. As shown in Fig. 3, the controlled current source is introduced into the two-branch model. The controlled current source is designed based on the SC terminal voltage and its change rate.

According to the relationship of $C = Q/U$, the self-discharge current $i_{\text{self-discharge}}(t)$ of the SC can be expressed as

$$i_{\text{self-discharge}}(t) = \frac{dQ}{dt} = C\frac{du(t)}{dt} = C\dot{u}(t) \tag{1}$$

where Q is the stored charge of the SC, $u(t)$ is the real-time SC terminal voltage, $\dot{u}(t)$ is the change rate of $u(t)$.

According to the Ohm's law, $i_{\text{self-discharge}}(t)$ can be also re-written as

$$i_{\text{self-discharge}}(t) = \frac{\Delta u(t)}{ESR} = \frac{-u_{\text{sc}}(t) + u(t)}{ESR} \tag{2}$$

where ESR is considered as the equivalent series resistance of the SC, $u_{\text{sc}}(t)$ is the open-circuit voltage of the SC.

Based on the above analyses, the current of the controlled current source can be assumed as a function related to the SC terminal voltage and its change rate

$$gu_s = A\dot{U}(s) + BU(s) \tag{3}$$

where gu_s is the current of the controlled current source, which is related to $i(t)$. $U(s)$ is the result of a Laplace transform of $u(t)$. $\dot{U}(s)$ is the change rate of $U(s)$. A and B are the coefficients of $\dot{U}(s)$ and $U(s)$, respectively. Both A and B are designed with positive constants.

With the controlled current source, the middle-term self-discharge behavior can be simulated effectively. What's more, the superposition current effect caused by the internal charge diffusion reaction (self-discharge process) in the SC can be also reflected. According to the charge-discharge and self-discharge experiments of the SC, it can be known that the controlled current source would present different parameter characteristics at different operating conditions of the SC. For the parameters (A and B) of the controlled current source, they can be identified by the recursive least square method. Therefore, using the controlled current source to describe the self-discharge characteristics of the SC can not only reduce the difficulty of the parameters identification for the parameter R_l, but also effectively describe the charge/discharge and self-discharge performance of the SC terminal voltage behavior in real time.

B. ANALYSIS OF THE SC SELF-DISCHARGE PHENOMENON AT DIFFERENT STAGES

For the SC, the self-discharge mechanism is very complex since different self-discharge performance would occur at different operating stages. On the other hand, the nonlinear characteristics of the SC self-discharge process are also affected by its initial voltage. Thus, the two parameters (A and B) of the controlled current source in the proposed model would be

discrepant at different operating stages. To achieve the parameters identification of the controlled current source, it should analyze the experimental data of the SC self-discharge during different operating stages. In the experiments, the minimum operating voltage of the SC is about 0.4 V. On the other hand, the self-recovery phenomenon of the terminal voltage of the SC is obvious when the terminal voltage is lower than 0.5 V. If the SC is discharged from 2.7 V to 0.5 V or 0.4 V, more than 96.5% or 97.8% of the SC stored energy would be delivered theoretically. Therefore, 0.5 V is set as the boundary value of the SC terminal voltage, and 0.4 V is set as the initial voltage of the SC.

Based on the experimental results in Fig. 2(c), the parameters A and B of the controlled current source in the proposed model would dynamically change depend on the charge, discharge and rest stages. It can be concluded as follows.

(1) When $u(t) > 0.5$ V, $i(t) \neq 0$, the self-discharge effect of the SC would be suppressed completely during rapid charge and discharge processes. The controlled current source keeps in open circuit state, and the parameters A and B are equal to 0. The improved model can be equivalent to the two-branch model in Fig. 2(a).

(2) When $u(t) > 0.5$ V, $i(t) = 0$, the SC terminal voltage drops obviously while the change rate of the terminal voltage fluctuates slightly during the static stage after the charge process. In this phase, the controlled current source should be used to compensate the terminal voltage particularly.

(3) When $u(t) \leq 0.5$ V, $i(t) \neq 0$, the change rate of the SC terminal voltage fluctuates strongly while the change of the SC terminal voltage is small after the end of discharge process. To modify the two-branch model, the controlled current source should be utilized to compensate the change rate of the SC terminal voltage.

(4) When $u(t) \leq 0.5$ V, $i(t) = 0$, the self-recovery phenomenon of SC terminal voltage would appear because of the slow charge diffusion reaction inside the SC during the static stage after discharge process. The SC terminal voltage would rise significantly and the change rate of the terminal voltage would fluctuate dramatically. To further describe the self-discharge performance of the SC at different stages, the controlled current source should be employed to compensate the change of the SC terminal voltage and its change rate simultaneously.

IV. MODEL PARAMETERS IDENTIFICATION

A. IDENTIFICATION OF THE MODEL PARAMETERS

The recursive least square algorithm is introduced to identify the parameters of the improved two-branch equivalent circuit model with the controlled current source in this paper. It has been demonstrated that the recursive least square algorithm can achieve high efficiency [34] and high accuracy [35] identification for the functions and parameters of the mathematical model. For the improved two-branch equivalent circuit model with the controlled current source of the SC, we select the operating current $i(t)$ as the input and the terminal voltage $u(t)$ as the output. The transfer function $G(s)$ of the proposed model can be calculated as follows

$$\begin{aligned} G(s) &= U(s)/(I(s)+gu_s) = U(s)/(I(s)+AsU(s)+BU(s)) \\ &= (b_2s^2 + b_1s + b_0)/(s^2 + a_1s + a_0) \end{aligned} \tag{4}$$

$$\begin{aligned} U(s)/I(s) = (b_2s^2+b_1s+b_0)/[-Ab_2s^3+(1-Ab_1-Bb_2)s^2 \\ +(a_1-Ab_0-Bb_1)s+(a_0-Bb_0)] \end{aligned} \tag{5}$$

The relationship between the capacitances and resistances can be calculated as

$$\begin{cases} a_1 = (R_iC_i + R_dC_d + R_lC_i + R_lC_d)/(XC_iC_d) \\ a_0 = 1/(XC_iC_d) \\ b_2 = (R_iR_dR_lC_iC_d)/(XC_iC_d) \\ b_1 = (R_iR_lC_i + R_dR_lC_d)/(XC_iC_d) \\ b_0 = R_l/(XC_iC_d) \\ X = R_iR_l + R_dR_l + R_iR_d \end{cases} \tag{6}$$

Based on the bilinear transformation, (5) is changed as

$$\begin{aligned} G(z) = (4b_2Txy^2+2b_1T^2x^2y+b_0T^3x^3)/[-8Ab_2y^3+4Txy^2 \\ (1-Ab_1-Bb_2)+2T^2x^2y(a_1-Ab_0-Bb_1)+T^3x^3(a_0-Bb_0)] \end{aligned} \tag{7}$$

where T is the sampling period, $\mathrm{x} = 1 + \mathrm{z}^{-1}$, $\mathrm{y} = 1 - \mathrm{z}^{-1}$.

The difference equation can be obtained based on (7)

$$\begin{aligned} u(z) &= \alpha_1u(z-1) + \alpha_2u(z-2) + \alpha_3u(z-3) + \beta_1i(z) \\ &+\beta_2i(z-1) + \beta_3i(z-2) + \beta_4i(z-3) \end{aligned} \tag{8}$$

where $\alpha_1, \alpha_2, \alpha_3, \beta_1, \beta_2, \beta_3, \beta_4$ are the correlation coefficients of the difference equations. $u(z)$, $i(z)$ are the output terminal voltage and the input current recorded by the experimental tester, respectively.

Define $Y = -(A+B)(b_2+b_1+b_0) + a_1 + a_0 + 1$, the relationship among the correlation coefficients of (7) and (8) can be expressed as

$$\begin{cases} \alpha_1 = -(3Ab_2 + Bb_2 + Ab_1 - Bb_1 - \\ \qquad Ab_0 - 3Bb_0 + a_1 + 3a_0 - 1)/Y \\ \alpha_2 = -(Bb_2 - 3Ab_2 + Ab_1 + Bb_1 \\ \qquad +Ab_0 - 3Bb_0 - a_1 + 3a_0 - 1)/Y \\ \alpha_3 = -(Ab_2 - Bb_2 + Bb_1 - Ab_1 \\ \qquad +Ab_0 - Bb_0 - a_1 + a_0 + 1)/Y \\ \beta_1 = (b_2 + b_1 + b_0)/Y, \quad \beta_2 = (-b_2 + b_1 + 3b_0)/Y \\ \beta_3 = (-b_2 - b_1 + 3b_0)/Y, \quad \beta_4 = (b_2 - b_1 + b_0)/Y \end{cases} \tag{9}$$

Based on (8), the data matrix of the experimental input-output $h(z)$ and the correlation coefficient matrix θ can be expressed as

$$\begin{aligned} h(z) = [&-u(z-1), -u(z-2), -u(z-3), \\ &i(z), i(z-1), i(z-2), i(z-3)] \end{aligned} \tag{10}$$

$$\theta = [-\alpha_1, -\alpha_2, -\alpha_3, \beta_1, \beta_2, \beta_3, \beta_4]^T \tag{11}$$

Finally, (8) can be rewritten as

$$u(z) = h(z)\theta \tag{12}$$

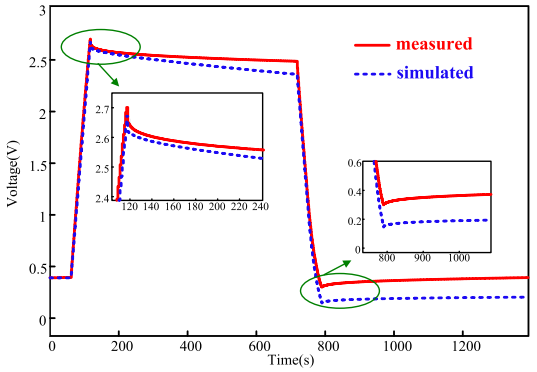

FIGURE 4. Comparison between the simulation and experimental results of the improved two-branch model based on the comprehensive values of the controlled current source.

According to (4) ∼ (12), the parameters A and B of the controlled current source, the resistances and capacitances in the equivalent circuit model can be identified by the recursive least square algorithm, respectively.

B. PARAMETERS OPTIMIZATION OF THE CONTROLLED CURRENT SOURCE

By using the recursive least square algorithm, we can obtain the comprehensive values of the controlled current source (A = 49.8998, B = 0.1102). However, it can be seen that the improved two-branch model has a large relative error with the comprehensive values of the controlled current source. Actually, the SC has different self-discharge performance in accordance with the operating stages. It is inaccuracy to describe the complex self-discharge effect of the SC with the comprehensive values of the controlled current source.

Based on the design of (3), we know that the parameter A is related to the change rate of the terminal voltage, and the parameter B is related to the real-time voltage response of the SC. The accuracy of the parameters A and B would directly affect the calculation accuracy of the improved two-branch equivalent circuit model with the controlled current source. On the other hand, we assume that the self-discharge effect has little relationship with the parameters of the conventional two-branch equivalent circuit model, since the controlled current source is used to reflect the self-discharge effect. This assumption is reasonable according to [23]. Therefore, it is necessary to optimize the parameters of the controlled current source.

Based on the parameters A and B identified and updated by the recursive least square algorithm at different times, many experiments and simulation tests are presented, as shown in Fig. 5 and Fig. 6. It should be noticed that the parameters A and B can be limited by using the updated identification results of recursive least square algorithm. For the parameter A of the controlled current source, if it is designed in the region 30-700, it can be seen from Fig 5(a) that simulation results are basically in accordance with the experimental results. There is no voltage fluctuation at charge stage. However, if the parameter A is higher than 83, the serious voltage

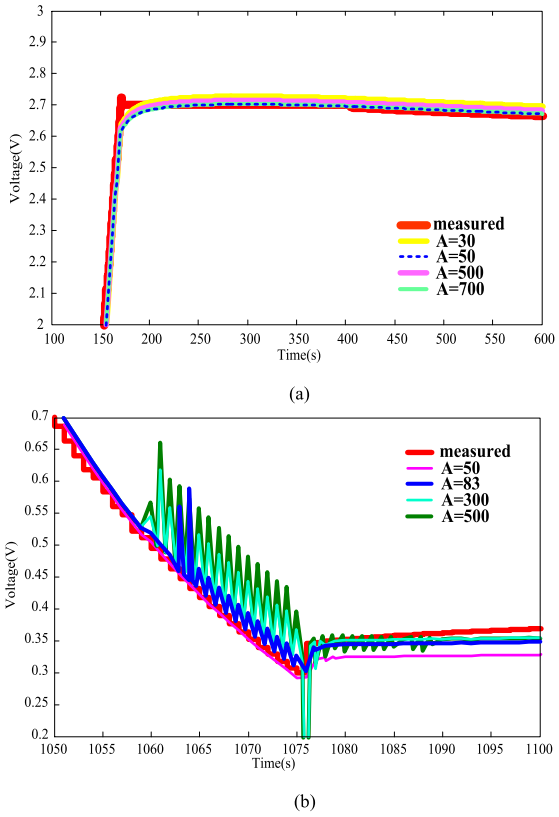

FIGURE 5. Influence based on the design of parameters A. (a) The self-discharge stage at the end of charging. (b) The self-discharge stage at the end of discharging.

fluctuation would occur at discharge stage and self-discharge stage after the end of discharging, as shown in Fig. 5(b).

For the parameter B of the controlled current source, the simulation results and experimental results are also consistent at charge stage when the parameter B changes from 0 to 0.3075, as show in Fig. 6(a). However, it can be seen from Fig. 6(b) that the simulated voltages are significant difference after the end of the discharge stage when the parameter B only changes slightly. To ensure the calculation accuracy of the parameter B of the controlled current source, a large number of the model analyses and experimental results are implemented. Results show that the model accuracy ($e \leq 0.01$) could be obtained when the change accuracy of the parameter B is within 0.01%.

Since the parameters A and B of the controlled current source would affect the calculation accuracy of the proposed model, they should be optimized or modified to assure the model precision. In this paper, based on the results identified by the recursive least square algorithm, the iterative optimization algorithm [36] is adopted to optimize the parameters A and B. The flow chart of the iterative optimization algorithm is shown in Fig. 7. The initial values A_0 and B_0 are obtained by the recursive least square algorithm. Then, the new parameters A and B are obtained based on repeated iteration of A_0 and B_0. The updated parameters are substituted into the improved two-branch equivalent circuit model with the controlled current source to acquire the new simulated SC

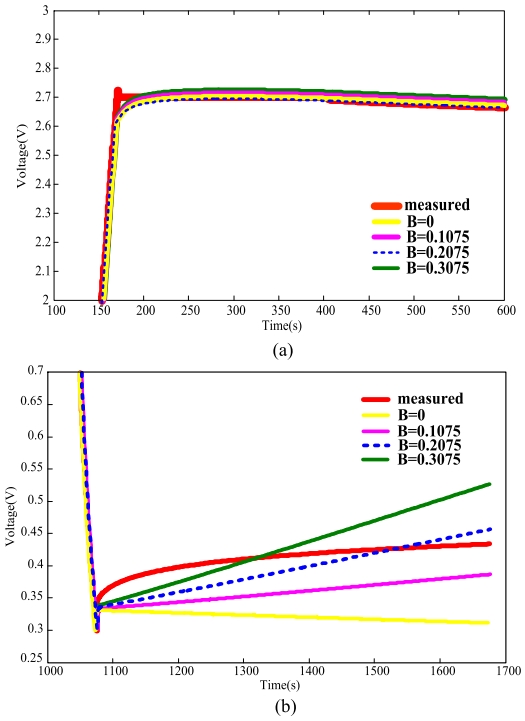

FIGURE 6. Influence based on the design of parameters B. (a) The self-discharge stage at the end of charging. (b) The self-discharge stage at the end of discharging.

terminal voltage. Finally, the new simulated terminal voltage results are compared with the actual experimental voltage until the relative error of the proposed model is less than 1% ($e \leq 0.01$). The average error is defined as the variance of the actual experimental output voltage and the simulated output voltage [28], it can be calculated as

$$error_{\text{ave}} = \frac{1}{n}\sum_{k=1}^{n}[u(k) - \hat{u}(k)]^2 \tag{13}$$

where $u(k)$ is the actual experimental output voltage, $\hat{u}(k)$ is the simulated output voltage of the SC.

Based on (13), the relative error of the proposed model is defined as

$$error_{\text{rel}} = \frac{1}{n}\sum_{k=1}^{n}[\frac{u(k) - \hat{u}(k)}{u(k)}]^2 \times 100\% \tag{14}$$

V. EXPERIMENT AND MODEL VALIDATION

A. EXPERIMENT AND PARAMETERS IDENTIFICATION RESULTS

The SC in the experiment is SAMWHA 350 F. The specific parameters of the SC are shown in Table 2. To validate the improved two-branch equivalent circuit model with the controlled current source and its parameters identification method, the experimental platform has been established, as shown in Fig. 8. Based on the Neware multi-channel tester CE-7002 and the monitoring system of the experimental platform, the experimental data can be obtained. The output voltage and input current curves of the SC are show in Fig. 9.

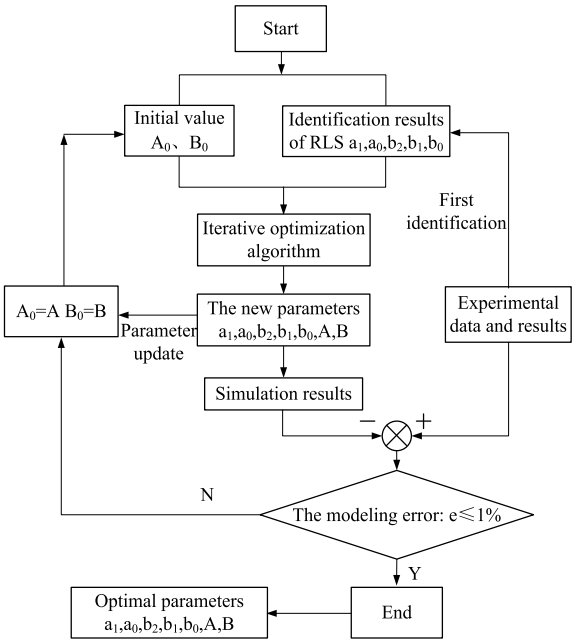

FIGURE 7. Flow chart of iterative optimization algorithm.

TABLE 2. The specific parameters of the SC.

Supercapacitor type	SAMWHA 350F
Rated voltage	2.7 V
Rated capacitance	350 F
Typical resistance	3.2~5.0 mΩ
Power density	4600 W/kg
Energy density	5.9 Wh/kg

FIGURE 8. Multi-channel test platform of the SC.

In Fig. 9, the charge/discharge current is designed as 15 A and the sampling period is designed as 1 s. The SC is charged to the rated voltage and then kept in static stage for 10 minutes. Finally, the discharge experiment is carried out until the SC terminal voltage decreases to the boundary value, and the SC is also kept in static stage for 10 minutes. According to the experimental data, the recursive least square algorithm is adopted to identify the parameters of the improved two-branch equivalent circuit model with the controlled current source. The identification results are shown in Table 3.

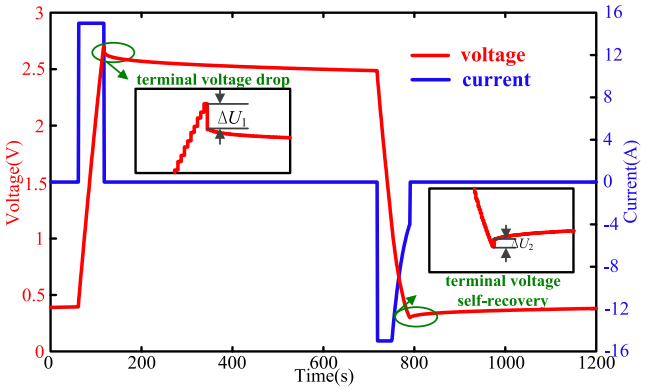

FIGURE 9. Experimental results (output voltage and input current curves) of the SC.

TABLE 3. Identification results of the improved two-branch equivalent circuit model with the controlled current source.

Parameters	Unit	Values
R_i	Ω	0.0045
R_d	Ω	0.0121
R_l	Ω	20.4340
C_{i0}	F	307.8939
C_{i1}	F/V	0.1248
C_d	F	60.3900
A	/	49.8998
B	/	0.1102

It can be seen from Fig. 9 that the SC terminal voltage rises or drops rapidly during the charge and discharge stages, respectively. Actually, the self-discharge effect is not so obvious during the charge and discharge stages. On the other hand, the SC terminal voltage rises and drops smoothly during the static stage after the charge and discharge stages since the self-discharge effect achieves the balance of the internal capacitance of the SC. Therefore, the parameters A and B of the controlled current source in the proposed model should be identified and optimized at different stages to compensate the self-discharge effect of the SC.

The iterative optimization algorithm is adopted to optimize and modify the parameters A and B of the controlled current source. By analyzing the influence degree of the parameters A and B on the SC terminal voltage and its change rate, the parameters A and B are continuously updated until the relative error of the proposed model is less than 1%. In this way, it can obtain the optimal identification results of the parameters A and B. Some identification results and the corresponding relative errors based on the iterative optimization algorithm are shown in Table 4. Finally, the identification results of parameters A and B at different operating stages are shown in Table 5.

B. MODEL VALIDATION

To verify the effectiveness of the improved two-branch equivalent circuit model with the controlled current source

TABLE 4. Comparative analyses of the identification results of parameters A and B.

Number of iterations	Identification results of parameter A	Identification results of parameter B	Relative errors
1	48.9978	0.1102	0.12%
4	49.8996	0.1250	0.11%
7	49.8997	0.1726	0.08%
10	49.9608	0.1864	0.08%
15	49.9993	0.2075	0.07%

TABLE 5. Identification results of the parameters A and B.

Operating conditions	Values
$u(t)>0.5$ V, $i(t)\neq 0$	A≈0, B≈0
$u(t)>0.5$ V, $i(t)=0$	A=49.9993, B=0.0502
$u(t)\leq 0.5$ V, $i(t)\neq 0$	A=48.6351, B=0.0012
$u(t)\leq 0.5$ V, $i(t)=0$	A=49.4168, B=0.2075

can describe the self-discharge characteristics of the SC, the charge-rest experiment, discharge-rest experiment, charge-rest-discharge-rest experiment and charge-discharge cycle experiment are implemented. The charge/discharge current is designed as 15 A. The experimental design of the operating conditions is the same as that of in part A of Section V. To make the improved two-branch equivalent circuit model with the controlled current source and its parameters identification method become more persuasive, the experiments of different charge and discharge depth for the SC are designed. First, the SC is charged to 2.5 V or 2.0 V. Then, the discharge tests are implemented until the voltage of the SC decreases to the boundary value of the SC terminal voltage. Finally, the comparative results are shown in Fig. 10.

From Fig. 10, the simulation results of the improved two-branch equivalent circuit model with the controlled current source are basically in accordance with the experimental results. The relative errors of the proposed model in multi-group experiments are calculated, as shown in Table 6. In addition, the proposed model is compared with the conventional two-branch model under different experimental conditions. The comparative results are shown in Table 7. The model precision can be improved up to 0.4% in the whole operation period when the SC is charged to the rated voltage. It can be seen from Table 6 and Table 7 that the proposed model can better reflect the charge/discharge and self-discharge performance of the SC when compared with the conventional two-branch model.

To verify the universal applicability of the improved two-branch equivalent circuit model with the controlled current source, the charge-rest experiment, discharge-rest experiment, charge-rest-discharge-rest experiment and charge-discharge cycle experiment are also implemented in

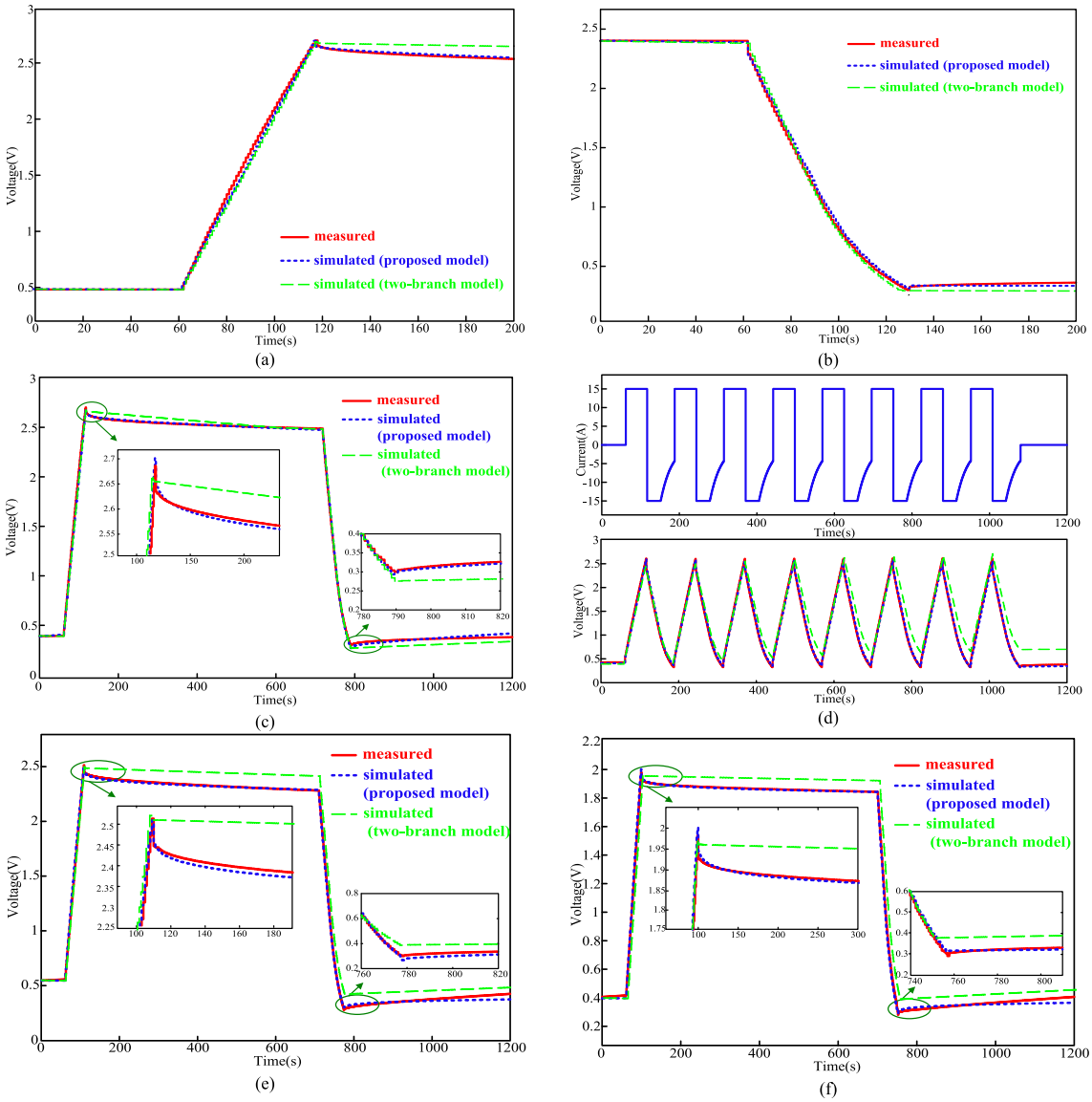

FIGURE 10. Comparison between the simulation and experimental results of the improved two-branch equivalent circuit model with the controlled current source when the operating current of the SC is designed as 15 A. (a) Charge-rest experiment. (b) Discharge-rest experiment. (c) Charge-rest-discharge-rest experiment (the SC is kept in static stage for 10 minutes). (d) Charge-discharge cycle experiment. (e) SC is charged to 2.5 V. (f) SC is charged to 2.0 V.

TABLE 6. The modeling errors in multi-group experiments.

Experimental type	Charge-rest experiment	Discharge-rest experiment	Charge-rest-discharge-rest experiment	Charge-discharge cycle experiment
Relative errors	0.11%	0.16%	0.29%	0.58%

the case of 10 A constant charge/discharge operating current. The comparative results of the experiment and simulation are shown in Fig. 11. For the experimental platform, it also has an equivalent resistance. When the SC is discharged at a low voltage, the voltage drop in the equivalent resistance of the experimental platform and the SC internal resistance would be close to the open-circuit voltage of the SC. So the SC cannot be discharged with a large current. As a result, the discharge current is reduced.

From Fig.11, the simulation results of the improved two-branch equivalent circuit model with the controlled current source and the experimental results are also consistent. Hence, the improved two-branch equivalent circuit model with the controlled current source can effectively describe the

TABLE 7. Comparison of the average output errors of different charge and discharge depth of the SC.

Multi-group experiments		Proposed model	Two-branch model
The SC is charged to 2.7 V	Self-discharge stage after charge	0.18%	0.22%
	Self-discharge stage after discharge	0.22%	1.07%
	Charge-rest-discharge-rest experiment	0.40%	1.78%
The SC is charged to 2.5 V	Self-discharge stage after charge	0.38%	2.35%
	Self-discharge stage after discharge	0.19%	1.13%
	Charge-rest-discharge-rest experiment	0.69%	2.56%
The SC is charged to 2.0 V	Self-discharge stage after charge	0.20%	1.72%
	Self-discharge stage after discharge	0.17%	0.19%
	Charge-rest-discharge-rest experiment	0.50%	1.42%

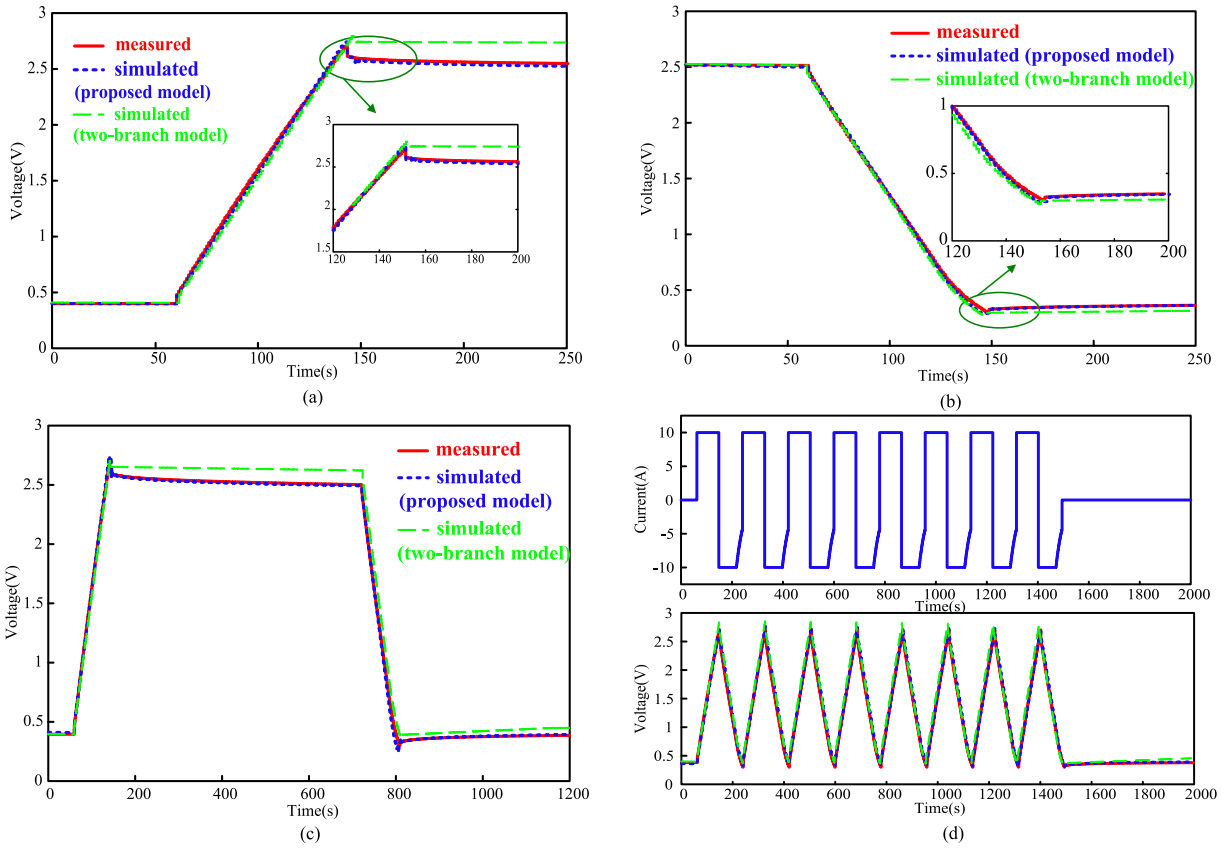

FIGURE 11. Comparison between the measured and simulation results of the improved two-branch equivalent circuit model with the controlled current source when the operating current of the SC is designed as 10 A. (a) Charge-rest experiment. (b) Discharge-rest experiment. (c) Charge-rest-discharge-rest experiment. (d) Charge-discharge cycle experiment.

SC dynamic behavior in both the charge/discharge phase and the rest phase. In practical applications, the proposed model would be valuable to enhance the control accuracy of the SC system.

VI. CONCLUSION

An improved two-branch equivalent circuit model with a controlled current source has been developed for describing the real-time charge/discharge and self-discharge operating characteristics of the SC. First, the experimental and simulation analyses showed that the conventional two-branch model could not effectively describe the self-discharge behavior of the SC. Therefore, the controlled current source was introduced to improve the conventional two-branch equivalent circuit model. Furthermore, to design the two parameters of the controlled current source, the self-discharge mechanism of the SC was studied by testing and analyzing the SC terminal voltage and its change rate at different operating stages. On this basis, the recursive least square method was adopted to identify the parameters of the improved

two-branch equivalent circuit model with the controlled current source. To improve the accuracy of the proposed model, the iterative optimization algorithm was adopted to optimize and modify the parameters of the controlled current source.

The simulation model based on the SC improved two-branch equivalent circuit with the controlled current source was established. Simulation results of the proposed model were compared with the experimental results. The simulation results of the proposed model are basically in accordance with the experimental results. It is shown that the proposed model can not only accurately reflect the real-time charge/discharge performance, but also reflect the self-discharge effect of the SC at different operating stages. The relative error of the proposed model was less than 0.7%. Compared with the conventional two-branch model, the proposed model can better reflect the self-discharge performance of the SC. Hence, the proposed model can effectively describe the SC dynamic behavior in both the charge/discharge phase and the rest phase.

REFERENCES

[1] N. Devillers, S. Jemei, M.-C. Péra, D. Bienaimé, and F. Gustin, "Review of characterization methods for supercapacitor modelling," *J. Power Sources*, vol. 246, pp. 596–608, Jan. 2014.

[2] A. González, E. Goikolea, J. A. Barrena, and R. Mysyk, "Review on supercapacitors: Technologies and materials," *Renew. Sustain. Energy Rev.*, vol. 58, pp. 1189–1206, May 2016.

[3] B. Wang, J. Xu, B. Cao, and B. Ning, "Adaptive mode switch strategy based on simulated annealing optimization of a multi-mode hybrid energy storage system for electric vehicles," *Appl. Energy*, vol. 194, pp. 596–608, May 2017.

[4] B. Wang, J. Xu, R.-J. Wai, and B. G. Cao, "Adaptive sliding-mode with hysteresis control strategy for simple multimode hybrid energy storage system in electric vehicles," *IEEE Trans. Ind. Electron.*, vol. 64, no. 2, pp. 1404–1414, Feb. 2017.

[5] M. Hassanalieragh, T. Soyata, A. Nadeau, and G. Sharma, "UR-SolarCap: An open source intelligent auto-wakeup solar energy harvesting system for supercapacitor-based energy buffering," *IEEE Access*, vol. 4, pp. 542–557, 2017.

[6] U. Akram, M. Khalid, and S. Shafiq, "An innovative hybrid wind-solar and battery-supercapacitor microgrid system—Development and optimization," *IEEE Access*, vol. 5, pp. 25897–25912, 2017.

[7] H. Yang and Y. Zhang, "Analysis of supercapacitor energy loss for power management in environmentally powered wireless sensor nodes," *IEEE Trans. Power Electron.*, vol. 28, no. 11, pp. 5391–5403, Nov. 2013.

[8] F. Ongaro, S. Saggini, and P. Mattavelli, "Li-ion battery-supercapacitor hybrid storage system for a long lifetime, photovoltaic-based wireless sensor network," *IEEE Trans. Power Electron.*, vol. 27, no. 9, pp. 3944–3952, Sep. 2012.

[9] V. Yuhimenko, G. Geula, G. Agranovich, M. Averbukh, and A. Kuperman, "Average modeling and performance analysis of voltage sensorless active supercapacitor balancer with peak current protection," *IEEE Trans. Power Electron.*, vol. 32, no. 2, pp. 1570–1578, Feb. 2016.

[10] R. Drummond, S. Zhao, D. A. Howey, and S. R. Duncan, "Circuit synthesis of electrochemical supercapacitor models," *J. Energy Storage*, vol. 10, pp. 48–55, Apr. 2017.

[11] Y. Parvini, J. B. Siegel, A. G. Stefanopoulou, and A. Vahidi, "Supercapacitor electrical and thermal modeling, identification, and validation for a wide range of temperature and power applications," *IEEE Trans. Ind. Electron.*, vol. 63, no. 3, pp. 1574–1585, Mar. 2016.

[12] C. F. Zou, L. Zhang, X. Hu, Z. Wang, T. Wik, and M. Pecht, "A review of fractional-order techniques applied to lithium-ion batteries, lead-acid batteries, and supercapacitors," *J. Power Sources*, vol. 390, pp. 286–296, Jun. 2018.

[13] L. Zhang, X. Hu, Z. Wang, F. Sun, and D. G. Dorrell, "A review of supercapacitor modeling, estimation, and applications: A control/management perspective," *Renew. Sustain. Energy Rev.*, vol. 81, pp. 1868–1878, Jan. 2017.

[14] T. Tevi and A. Takshi, "Modeling and simulation study of the self-discharge in supercapacitors in presence of a blocking layer," *J. Power Sources*, vol. 273, pp. 857–862, Jan. 2015.

[15] A. Lewandowski, P. Jakobczyk, M. Galinski, and M. Biegun, "Self-discharge of electrochemical double layer capacitors," *Phys. Chem. Chem. Phys.*, vol. 15, no. 22, pp. 8692–8699, Dec. 2013.

[16] H. Yang and Y. Zhang, "Self-discharge analysis and characterization of supercapacitors for environmentally powered wireless sensor network applications," *J. Power Sources*, vol. 196, no. 20, pp. 8866–8873, 2011.

[17] Y. Zhang and H. Yang, "Modeling and characterization of supercapacitors for wireless sensor network applications," *J. Power Sources*, vol. 196, no. 8, pp. 4128–4135, 2011.

[18] J. Kowal *et al.*, "Detailed analysis of the self-discharge of supercapacitors," *J. Power Sour.*, vol. 196, no. 1, pp. 573–579, 2011.

[19] M. Kaus, J. Kowal, and D. U. Sauer, "Modelling the effects of charge redistribution during self-discharge of supercapacitors," *Electrochim. Acta*, vol. 55, pp. 7516–7523, Oct. 2010.

[20] H. Yang and Y. Zhang, "A task scheduling algorithm based on supercapacitor charge redistribution and energy harvesting for wireless sensor nodes," *J. Energy Storage*, vol. 6, pp. 186–194, May 2016.

[21] H. Yang and Y. Zhang, "A study of supercapacitor charge redistribution for applications in environmentally powered wireless sensor nodes," *J. Power Sources*, vol. 273, pp. 223–236, Jan. 2015.

[22] S.-H. Kim, W. Choi, K.-B. Lee, and S. Choi, "Advanced dynamic simulation of supercapacitors considering parameter variation and self-discharge," *IEEE Trans. Power Electron.*, vol. 26, no. 11, pp. 3377–3385, Nov. 2012.

[23] D. Torregrossa, M. Bahramipanah, E. Namor, R. Cherkaoui, and M. Paolone, "Improvement of dynamic modeling of supercapacitor by residual charge effect estimation," *IEEE Trans. Ind. Electron.*, vol. 61, no. 3, pp. 1345–1354, Mar. 2014.

[24] D. Xu, L. Zhang, B. Wang, and G. L. Ma, "A novel equivalent-circuit model and parameter identification method for supercapacitor performance," *Energy Procedia*, vol. 145, pp. 133–138, Apr. 2018.

[25] R. Faranda, "A new parameters identification procedure for simplified double layer capacitor two-branch model," *Elect. Power Syst. Res.*, vol. 80, no. 4, pp. 363–371, 2010.

[26] P. O. Logerais *et al.*, "Modeling of a supercapacitor with a multi-branch circuit," *Int. J. Hydrogen Energy*, vol. 40, pp. 13725–13736, Oct. 2015.

[27] R. German, A. Hammar, R. Lallemand, A. Sari, and P. Venet, "Novel experimental identification method for a supercapacitor multipore model in order to monitor the state of health," *IEEE Trans. Power Electron.*, vol. 31, no. 1, pp. 548–559, Jan. 2016.

[28] C.-T. Goh and A. Cruden, "Bivariate quadratic method in quantifying the differential capacitance and energy capacity of supercapacitors under high current operation," *J. Power Sources*, vol. 265, pp. 291–298, Nov. 2014.

[29] H. Yang and Y. Zhang, "Characterization of supercapacitor models for analyzing supercapacitors connected to constant power elements," *J. Power Sources*, vol. 312, pp. 165–171, Apr. 2016.

[30] J.-F. Shen, Y.-J. He, and Z.-F. Ma, "A systematical evaluation of polynomial based equivalent circuit model for charge redistribution dominated self-discharge process in supercapacitors," *J. Power Sources*, vol. 303, pp. 294–304, Jan. 2016.

[31] R. Chai, H. Ying, and Y. Zhang, "Supercapacitor charge redistribution analysis for power management of wireless sensor networks," *IET Power Electron.*, vol. 10, pp. 169–177, Feb. 2017.

[32] N. Bertrand, J. Sabatier, O. Briat, and J. M. Vinassa, "Embedded fractional nonlinear supercapacitor model and its parametric estimation method," *IEEE Trans. Ind. Electron.*, vol. 57, no. 12, pp. 3991–4000, Dec. 2010.

[33] R. Chaari, O. Briat, and J.-M. Vinassa, "Capacitance recovery analysis and modelling of supercapacitors during cycling ageing tests," *Energy Convers. Manag.*, vol. 82, pp. 37–45, Jun. 2014.

[34] N. Reichbach and A. Kuperman, "Recursive-least-squares-based real-time estimation of supercapacitor parameters," *IEEE Trans. Energy Convers.*, vol. 31, no. 2, pp. 810–812, Jun. 2016.

[35] M. Pucci, G. Vitale, G. Cirrincione, and M. Cirrincione, "Parameter identification of a Double-Layer-Capacitor 2-branch model by a least-squares method," in *Proc. Conf. IEEE Ind. Electron. Soc.*, vol. 20, pp. 6770–6776, Nov. 2014.

[36] S. Kim and P. H. Chou, "Size and topology optimization for supercapacitor-based sub-watt energy harvesters," *IEEE Trans. Power Electron.*, vol. 28, no. 4, pp. 2068–2080, Apr. 2013.

DAN XU received the Ph.D. degree in mechanical engineering from Xi'an Jiaotong University, Xi'an, China, in 2013, where she is currently a Professor and the Director of the Department of Mechanical Engineering. Her research interests include battery systems, electric vehicles, supercapacitor modeling, dc–dc converter control, and motor control.

LE ZHANG was born in Henan, China, in 1992. She received the B.S. degree in vehicle engineering from Chang'an University, Xi'an, China, in 2016. She is currently pursuing the M.S. degree with the School of Mechanical Engineering, Xi'an Jiaotong University. Her research interests include supercapacitor modeling and management.

BIN WANG was born in Guangxi, China, in 1987. He received the B.S. degree in automation engineering and the M.S. degree in control science and engineering from the Henan University of Science and Technology, Luoyang, China, in 2010 and 2013, respectively, and the Ph.D. degree in mechanical engineering from Xi'an Jiaotong University, Xi'an, China, in 2017, where he is currently a Research Assistant with the School of Mechanical Engineering. His research interests include energy storage systems, electric vehicles, dc–dc converter control, and supercapacitor state-of-charge estimation.

GUANGLIANG MA was born in Henan, China, in 1994. He received the B.S. degree in information engineering from Xi'an Jiaotong University, Xi'an, China, in 2016, where he is currently pursuing the M.S. degree with the School of Mechanical Engineering. His research interests include electric vehicle energy management and dc–dc converter control.